

Observation of Quantum Paraelectricity in an Intermolecular Ionic Hydrogen-Bonded Crystal of a Squaric Acid Derivative

Isao Takasu, Akira Izuoka,[†] and Tadashi Sugawara*

Department of Basic Science, Graduate School of Arts and Sciences, The University of Tokyo, Komaba, Meguro-ku, Tokyo 153-8902, Japan

Tomoyuki Mochida

Department of Chemistry, Faculty of Science, Toho University, Miyama, Funabashi, Chiba 274-8510, Japan

Received: August 7, 2003; In Final Form: January 12, 2004

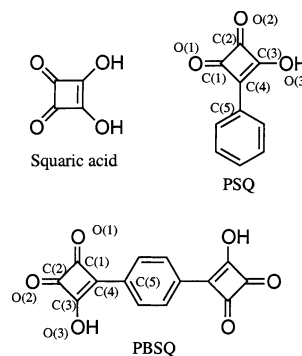
Proton transfer in a hydrated crystal of a squaric acid derivative, *p*-phenylenebis(squaric acid) (PBSQ), was investigated by means of ac dielectric measurements. The crystal consisted of PBSQ monoanions and protonated water dimer (H_5O_2^+) counter cations, and a highly symmetric, one-dimensional hydrogen-bonded chain was formed through strong $\text{OH} \cdots \text{O}^-$ ionic hydrogen bonding between deprotonated PBSQ moieties. The permittivity of the hydrated crystal was nearly temperature independent ($\epsilon' \sim 9$), but the deuterated crystal exhibited a Curie–Weiss type temperature dependence and underwent depression of the permittivity at 28 K, which is the characteristic of an (anti)ferroelectric phase transition. Thus, we conclude that the dielectric response of the hydrated PBSQ crystal originates from proton transfer along the intermolecular hydrogen bond and that the temperature-independent dielectric behavior can be interpreted in terms of quantum paraelectricity.

I. Introduction

Proton tunneling in the double-well potential of gas-phase malonaldehyde and its analogues has been investigated theoretically¹ and experimentally.^{2,3} We have found that quantum-mechanical tunneling also occurs in the intramolecular hydrogen-bonded crystal of 5-bromo-9-hydroxyphenalenone (BHP),^{4,5} which exhibits a symmetrical double-well type proton potential with a low barrier. In our study of the BHP crystal, we evaluated the degree of tunneling by heat capacity measurements⁶ and far-infrared spectroscopy.⁷ Squaric acid forms an organic two-dimensional hydrogen-bonded system in the crystalline state.⁸ Crystalline squaric acid shows an (anti)ferroelectric–paraelectric phase transition at about 375 K, associated with the order–disorder transition of the proton sites.⁹ In the two-dimensional hydrogen-bonded crystal of squaric acid, protons are considered to have a heavy effective mass, since they must migrate in accord with the relocation of the adjacent protons in the hydrogen-bonded network and also with the change of the π -conjugated structure of the squaryl groups. Under high pressure, however, the transition temperature is lowered in accord with the shortening of the hydrogen-bond length. Above 3 GPa, the transition is entirely suppressed, and a pronounced dielectric response is observed even at cryogenic temperatures. This phenomenon is interpreted in terms of *quantum paraelectricity*, derived from the quantum motion of a proton along the hydrogen bond.¹⁰ In our study, the BHP crystal, a zero-dimensional hydrogen-bonded system, also shows quantum paraelectricity under ambient pressure, and its deuterated crystal shows an (anti)ferroelectric transition (deuteron-induced phase

transition).^{4,5} In addition to the mentioned organic systems, some inorganic zero-dimensional hydrogen-bonded systems, for example, $\text{K}_3\text{H}(\text{SO}_4)_2$,^{11,12} exhibit similar quantum dielectric behavior in the solid state.

Under such a circumstance, it would be intriguing to observe a quantum dielectric phenomenon in an organic one-dimensional hydrogen-bonded crystalline system under ambient pressure. Thus, we prepared a one-dimensional hydrogen-bonded crystal of phenylsquaric acid, in which one of the hydroxy groups of squaric acid is replaced with a phenyl group. Crystalline phenylsquaric acid (PSQ), however, does not exhibit any proton dynamics along the hydrogen-bonded chain. This is partially due to the relatively long distance ($\text{O} \cdots \text{O}$, 2.618(2) Å) and the low symmetry of the hydrogen bond in the crystal.



Taking the above cases into consideration, two strategies emerge for observing proton tunneling along a hydrogen-bonded chain: first, formation of strong hydrogen bonds of high symmetries between hydrogen-bonding building blocks and, second, weakening of the intramolecular electronic correlation between a proton-donating site and a proton-accepting site

* Corresponding author. Fax: +81-3-5454-6997. E-mail: suga@pentacle.c.u-tokyo.ac.jp.

[†] Present address: Department of Materials and Biological Sciences, Faculty of Science, Ibaraki University, 2-1-1 Bunkyo, Mito, Ibaraki 310-8512, Japan.

within a tautomeric molecule. *p*-Phenylenebis(squaric acid) (PBSQ) was prepared as a model compound for observing the proton dynamics along a one-dimensional intermolecular hydrogen-bonded chain for the following reasons: (1) The molecular symmetry of PBSQ is reasonably high (C_{2h}), provided that the molecular structure is planar. (2) The squaric acid moieties are nearly independent electronically because they are separated by a *p*-phenylene unit; protonation or deprotonation at one of the squaric moieties does not significantly affect the acidity of the other. Here we report the proton dynamics of crystalline hydrated PBSQ.

II. Experimental Section

A. Preparation of Squaric Acid Derivatives. Phenylsquaric acid (PSQ) was synthesized by the coupling of iodobenzene and 3-(tri-*n*-butylstannyl)-4-isopropoxy-3-cyclobutene-1,2-dione,¹³ followed by deprotection with hydrochloric acid (yield 92%). Single crystals were obtained by slow evaporation from aqueous solution at room temperature. The crystal was a colorless prism (the largest crystal was $\sim 0.5 \times 0.2 \times 0.1$ mm³).

p-Phenylenebis(squaric acid) (PBSQ) was synthesized by the coupling of diiodobenzene and 3-(tri-*n*-butylstannyl)-4-isopropoxy-3-cyclobutene-1,2-dione, followed by deprotection with hydrochloric acid (yield 89%). Single crystals were obtained by slow evaporation from a 5% aqueous solution of trifluoromethanesulfonic acid at room temperature. The crystal was a yellow plate (the largest crystal was $\sim 2.0 \times 0.8 \times 0.08$ mm³). The $\sim 100\%$ deuterated PBSQ crystal was prepared by recrystallization from 99.8% deuterium oxide at room temperature in the first run, followed by recrystallization from a 5% solution of trifluoromethanesulfonic acid-*d* (98%) in deuterium oxide (99.8%) at room temperature in the second run. The $\sim 50\%$ deuterated PBSQ crystal was prepared by recrystallization from 50% deuterated water in the first run, followed by recrystallization from a 5% aqueous solution of trifluoromethanesulfonic acid at room temperature in the second run. The deuterium contents of the crystals were estimated to be the same as the deuterium contents of the solutions used for the recrystallizations.

B. X-ray Structure Analyses. The X-ray structure analyses were performed with Rigaku AFC-5 and Rigaku AFC-7R diffractometers for PSQ and PBSQ, respectively, using Mo K α radiation. The data were collected at 298 K using the ω -2 θ scan technique to a maximum 2 θ value of 55.0°. Crystal data and data collection parameters for PSQ and PBSQ are listed in Table 1. Selected bond lengths and angles are listed in Table 2. All calculations were performed with the teXsan crystallographic software package (Molecular Structure Corp.). Calculations were carried out on a Silicon Graphics INDY system.

Crystallographic data (excluding structure factors) for the structures in this paper have been deposited with the Cambridge Crystallographic Data Centre as supplementary publication nos. CCDC 189458 (PSQ) and 207519 (PBSQ). Copies of the data can be obtained, free of charge, upon application to CCDC, 12 Union Road, Cambridge CB2 1EZ, U.K. (fax, +44 1223 336033; e-mail, deposit@ccdc.cam.ac.uk).

C. Solid-State ¹³C NMR (CP/MAS) Spectra. High-resolution solid-state ¹³C NMR (CP/MAS) spectra were recorded on a Chemagnetics CMX300-NMR spectrometer at 75.6 MHz with a spinning rate of 4700 Hz. The data acquisition conditions were as follows: spectral width, 40 kHz; proton 90° pulse, 5 ms; cross polarization time, 5 ms; spectral width, 40 kHz; recycle delay, 10 s; number of acquisitions, 1000. Chemical shifts were externally referenced to the methyl carbons of hexamethylbenzene ($\delta = 17.35$ ppm).

TABLE 1: Crystallographic Parameters for PSQ and PBSQ

	PSQ	PBSQ
empirical formula	C ₁₀ H ₆ O ₃	C ₁₄ H ₁₀ O ₈
formula weight	174.15	306.23
crystal dimensions/mm	0.50 × 0.22 × 0.10	0.60 × 0.50 × 0.08
crystal system	triclinic	triclinic
space group	<i>P</i> 1 (No. 2)	<i>P</i> 1 (No. 2)
<i>a</i> /Å	7.177(2)	8.113(1)
<i>b</i> /Å	9.343(2)	8.119(2)
<i>c</i> /Å	6.494(2)	5.3235(7)
α /deg	101.67(2)	96.55(1)
β /deg	102.47(3)	96.02(1)
γ /deg	105.71(2)	112.90(1)
<i>V</i> /Å ³	393.2(2)	316.6(1)
<i>Z</i>	2	1
<i>D</i> _{calc} /(g cm ⁻³)	1.471	1.606
μ /cm ⁻¹	1.10	1.35
measured reflections	2793	1552
independent reflections	1391	1249
(<i>I</i> > 3 σ)		
<i>R</i> ₁ ^a	0.0426	0.038
<i>R</i> _w ^b	0.0412	0.138
GOF	1.8	1.1

$$^a R_1 = \sum ||F_o| - |F_c|| / \sum |F_o|. \quad ^b R_w = [\sum w(F_o^2 - F_c^2)^2 / \sum w(F_o^2)^2]^{1/2}.$$

TABLE 2: Selected Bond Distances (in Angstroms) and Bond Angles (in Degrees) for PSQ and PBSQ

PSQ			
O(1)–C(1)	1.218(2)	C(1)–C(4)	1.469(2)
O(2)–C(2)	1.201(2)	C(2)–C(3)	1.485(2)
O(3)–C(3)	1.302(2)	C(3)–C(4)	1.383(2)
C(1)–C(2)	1.531(2)	C(4)–C(5)	1.455(2)
O(3)–H(O(3))	0.95(2)		
C(1)–C(2)–C(3)	85.3(1)	O(2)–C(2)–C(1)	137.7(2)
C(2)–C(1)–C(4)	88.9(1)	O(3)–C(3)–C(2)	135.3(2)
C(2)–C(3)–C(4)	94.2(1)	C(1)–C(4)–C(5)	136.3(1)
C(1)–C(4)–C(3)	91.5(1)		
PBSQ			
O(1)–C(1)	1.229(2)	C(1)–C(4)	1.444(2)
O(2)–C(2)	1.209(2)	C(2)–C(3)	1.501(2)
O(3)–C(3)	1.263(2)	C(3)–C(4)	1.414(2)
C(1)–C(2)	1.515(2)	C(4)–C(5)	1.448(2)
O(1)–H(O(1))	1.239(1)		
C(1)–C(2)–C(3)	86.7(1)	O(1)–C(1)–C(4)	136.9(2)
C(1)–C(4)–C(3)	92.8(1)	O(2)–C(2)–C(3)	137.2(2)
C(2)–C(3)–C(4)	91.1(1)	O(3)–C(3)–C(4)	134.1(2)
C(2)–C(1)–C(4)	89.4(1)	C(3)–C(4)–C(5)	133.9(2)

D. Measurement of ac Dielectric Permittivity. The temperature dependence of the dielectric permittivity was measured with a Hewlett-Packard 4274A LCR meter in the frequency range 1×10^3 to 100×10^3 Hz for alternating electric fields of ~ 10 V/cm. Both sides of the sample (a very thin plate-shaped crystal of PBSQ (thickness ~ 0.08 mm)) were painted with conductive gold paste to allow electrical measurement. The temperature of the sample was measured with a Au/Fe chromel thermocouple. The anisotropy of the permittivity was not measured, owing to the thinness of the crystal.

III. Results and Discussion

A. Characteristics of the Hydrogen-Bonded Crystal of Phenylsquaric Acid (PSQ). In the PSQ crystal, the PSQ molecules form a chain structure along the *c*-axis through intermolecular hydrogen bonding between a hydroxy group and a carbonyl group of the adjacent molecule (Figure 1 and Tables 1 and 2). The hydrogen-bond O \cdots O distance in the PSQ crystal is 2.618(2) Å (the bond length of O–H, 0.95 Å; the bond angle of O–H \cdots O, 163(1)°), which is longer than that in the squaric acid crystal (2.55 Å). The phenyl group of PSQ is twisted 6.8–(4)° from the plane of the squaric acid moiety. The two planar groups in the unit cell are stacked alternately in a head-to-tail

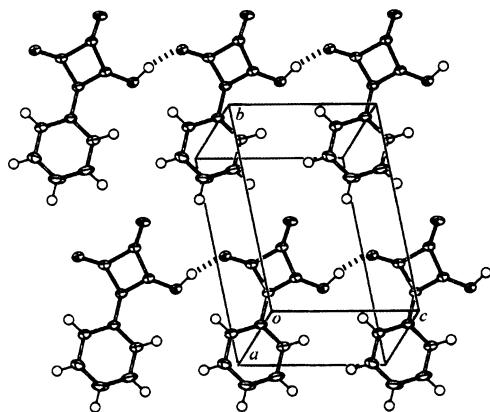


Figure 1. ORTEP-3 [27] diagram of the crystal structure of PSQ molecules forming one-dimensional hydrogen-bonded chains. The molecules are stacked along the *a*-axis. Thermal ellipsoids are drawn at 30% probability. The hydrogen bonds are shown by the dashed lines.

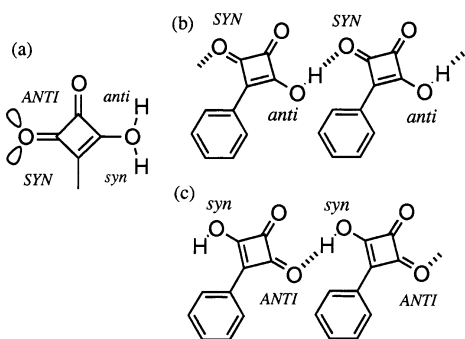


Figure 2. Definition of (a) the configuration of the hydrogen-bonding pattern of the squaric acid moiety, (b) the configuration of the hydrogen-bonding pattern of the PSQ crystal, and (c) the configuration of the hydrogen-bonding pattern of the PSQ crystal after hypothetical proton transfer.

manner along the *a*-axis. The C—O bond lengths corresponding to the enol and carbonyl groups are 1.302(2) and 1.218(2) Å, respectively. The C(1)—C(4) and —C(4)—C(3) bond lengths are 1.469(2) Å and 1.383 Å, respectively. The O—H bond length of PSQ is 0.95(2) Å. In general, the bond alternation in the π -conjugated system and the O—H bond length are closely correlated to the degree of localization of a proton in a hydrogen bond. On the other hand, in the X-ray analysis of the paraelectric phase of the squaric acid, the bond alternation in the π -conjugated system is diminished and the molecular skeleton shows D_{4h} symmetry.⁸ These results indicate that, in the PSQ crystal, the protons in the hydrogen bonds are localized.

The high-resolution solid-state ^{13}C NMR (CP/MAS) spectrum of PSQ recorded at room temperature was consistent with the foregoing results. The enol and carbonyl carbons, especially, resonated at different positions (190 and 197 ppm, respectively), and the line shape did not change even when the temperature was increased to 373 K. The experimental data confirmed the absence of a rapid exchange process (faster than $2 \times 10^3 \text{ s}^{-1}$) between intermolecular proton sites. Because proton transfer along the intermolecular hydrogen-bonded network of the PSQ crystal is strongly coupled with the π -bond switching in the squaryl group, the protons in the one-dimensional hydrogen-bonded chain in the PSQ crystal have a heavy effective mass. It should be noted that the hydrogen-bonding pattern of the PSQ crystal is of the *syn*—*anti* type^{14,15} (Figure 2b). If the correlated proton transfer occurs along the hydrogen bond, the hydrogen-bonding pattern changes to the *anti*—*syn* type (Figure 2c). Therefore, the hydrogen-bond structure of the PSQ crystal is asymmetric.

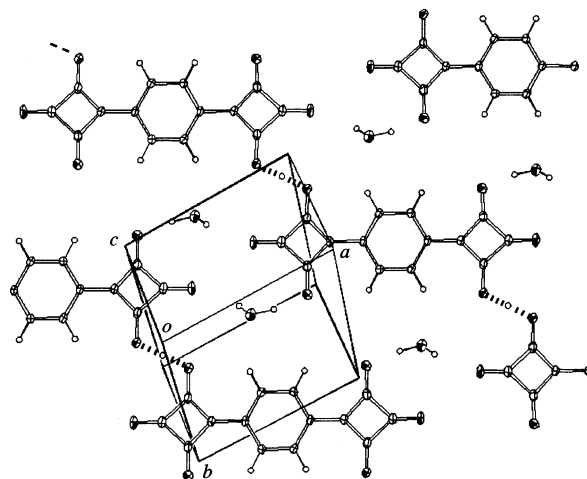


Figure 3. ORTEP-3 [27] diagram of the sheet structure of the PBSQ crystal. Thermal ellipsoids are drawn at 30% probability. The hydrogen bonds between the PBSQ molecules are shown by the dashed lines.

The major factor for the proton dynamics is the height of the potential barrier in the hydrogen bond. The potential barrier becomes low when the hydrogen-bond length is short and the intermolecular electrostatic or electronic interaction between the surrounding molecules is small. Furthermore, a symmetric hydrogen bond may induce the tunneling effect of the protons. In the PSQ crystal, however, the hydrogen-bond length is longer and the shape of the hydrogen bond is less symmetric compared with the case of the squaric acid crystal. These results are consistent with the fact that the hydrogen-bonded chain of the PSQ crystal does not exhibit a dynamic property.

B. Crystal Structure of Hydrated *p*-Phenylenebis(squaric acid) (PBSQ). Crystallization of PBSQ from a 5% aqueous solution of trifluoromethanesulfonic acid afforded one-dimensional hydrogen-bonded PBSQ crystals composed of PBSQ^- (monoanionic PBSQ) and H_5O_2^+ . The $\text{PBSQ}^- \cdot \text{H}_5\text{O}_2^+$ crystal is characterized by a layered structure (space group *P1*) (Figure 3 and Tables 1 and 2). In the unit cell of $\text{PBSQ}^- \cdot \text{H}_5\text{O}_2^+$, one PBSQ molecule and two water molecules are incorporated and each PBSQ molecule has only one hydrogen atom per two hydroxy groups, indicating that PBSQ exists as a monoanion. On the other hand, the water molecules in the crystal exist as protonated water dimers (H_5O_2^+), where the two water molecules are strongly linked by an excess bridging proton ($\text{H}_2\text{O} \cdots \text{H}^+ \cdots \text{OH}_2$).

Such deprotonation of acids and generation of oxonium ions (such as H_3O^+ and H_5O_2^+) in crystals has been reported for the hydrated crystals of strong acids.^{16,17} Squaric acid is known as a strong oxoacid ($\text{p}K_{\text{a}1} = 0.54$ and $\text{p}K_{\text{a}2} = 3.48$), and strong acidity of PSQ is also reported ($\text{p}K_{\text{a}} = -0.22$).¹⁸ Therefore, the PBSQ molecule is estimated to have strong acidity ($\text{p}K_{\text{a}1} < 1$) and the hydroxy group is deprotonated to form an oxonium ion in a hydrated crystal. In the case of squaric acid, various crystal structures of monohydrogen squarates have been reported.^{19,20}

Since PBSQ^- is located at the center of the inversion symmetry, a symmetrical, one-dimensional, ionic hydrogen-bonded chain consisting of PBSQ^- is constructed on the layer (Figure 4a). Ionic hydrogen bonds such as $\text{O}^- \cdots \text{H}-\text{O}$ and $\text{O} \cdots \text{H}-\text{O}^+$ are known to be very strong with a short hydrogen-bond length,¹⁷ owing to the strong electrostatic interaction. The hydrogen-bond $\text{O} \cdots \text{O}$ distance in the one-dimensional chain composed of PBSQ^- is 2.478(1) Å (the bond lengths of C—O and O—H are 1.263(2) and 1.239(1) Å, respectively), even

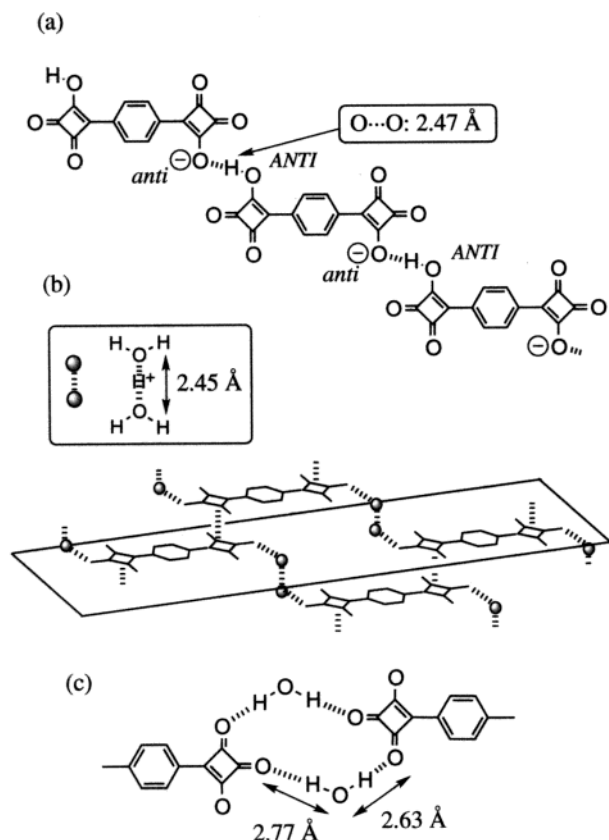


Figure 4. (a) Schematic structure of the one-dimensional hydrogen-bonded chain in the PBSQ crystal. The configuration of the hydrogen-bonding pattern of the PBSQ crystal is indicated. (b) Schematic structure of H_5O_2^+ in the PBSQ crystal. The hydrogen bond within H_5O_2^+ is directed perpendicular to the sheet. The hydrogen bonds between PBSQ^- and H_5O_2^+ are shown by the dashed lines. (c) Hydrogen bonds between the water molecules and the PBSQ molecules. The $\text{O} \cdots \text{O}$ distances are indicated.

shorter than that in the squaric acid crystal ($\text{O} \cdots \text{O}$, 2.55 Å). As for the counter ion, the axis of the hydrogen bond connecting the two water molecules in H_5O_2^+ is located perpendicular to the layer (Figure 4b), and the bridging proton is situated between the layers, although the proton is not shown in Figure 4b. The $\text{O} \cdots \text{O}$ distance in H_5O_2^+ is only 2.443(2) Å (the O—H bond length is 1.222(1) Å). The hydrogen atoms of two water molecules in H_5O_2^+ form hydrogen bonds also with two carbonyl groups of the PBSQ molecules ($\text{O} \cdots \text{O}$, 2.633(2) and 2.761(2) Å) on layers above and below, connecting them to the PBSQ^- chains within the layer, respectively (Figure 4c).

As described in the preceding paragraph, there are two strong hydrogen bonds: one is formed between PBSQ^- ions, and the other is within H_5O_2^+ . In the crystal, half of the PBSQ molecule is crystallographically independent, and the symmetrical center is at the center of the phenylene ring. Moreover, symmetrical centers are located at the middle of the hydrogen bond between the squaric acid moieties and at the middle of the hydrogen bond between the water molecules (H_5O_2^+). The hydrogen atoms in the hydrogen bonds above-mentioned are refined as a single hydrogen located at the center of the hydrogen bond, because both of them were not able to separate by the difference Fourier syntheses. Therefore, whether or not the hydrogen is in a double-well potential or in a single-well potential cannot be judged from the X-ray analyses. These results, however, indicate that the hydrogen-bond potential in this crystal is symmetrical and the barrier to proton transfer should be relatively low. Incidentally, the quantum effect on the proton transfer in H_5O_2^+

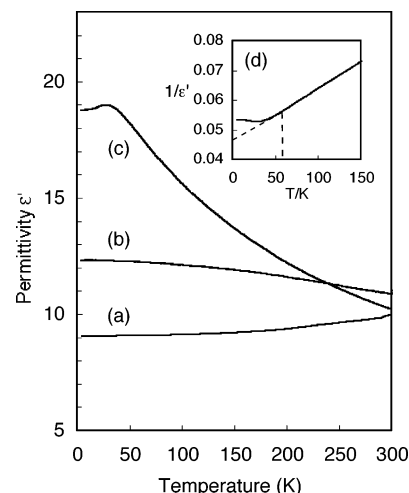


Figure 5. Deuteration effect on the temperature dependence of the permittivities (10 kHz) of the PBSQ crystal: (a) nondeuterated crystal; (b) ~50% deuterated crystal; (c) ~100% deuterated crystal; (d) Curie–Weiss behavior of the ~100% deuterated crystal.

has been investigated both theoretically and experimentally as the simplest model for proton transfer in water.^{21–24} Accordingly, the protons in the PBSQ crystal are expected to be dynamically disordered with respect to the location of the proton in the symmetric, strong hydrogen bond.

C. Temperature Dependence of the Dielectric Permittivities of PBSQ·2H₂O and the Deuterated Crystals. The temperature dependence of the ac dielectric permittivity of the hydrated PBSQ crystal was measured on an LCR meter over the temperature range 4–300 K (Figure 5a). The permittivity of the hydrated PBSQ crystal remained almost constant ($\epsilon' \sim 9$) over the temperature range 4–300 K, with no frequency dependence (1–100 kHz). Because the crystals are very thin plates (thickness ~ 0.08 mm), the alternating electric field was applied only along the [110] direction. Thus, the anisotropy of the permittivity could not be measured.

The effect of deuteration on the temperature dependence of the ac permittivity was examined. The permittivity of the ~100% deuterated sample increased with decreasing temperature, obeying the Curie–Weiss law over 60 K (Figure 5c,d). At temperatures lower than 28 K, the permittivity decreased slightly (Figure 5c). The Curie–Weiss behavior and the decrease in the permittivity are characteristic of the (anti)ferroelectric phase transition. The results can be rationalized by the fact that the deuterons in the strong hydrogen bonds are ordered at 28 K by the antiferroelectric interaction between the hydrogen-bonded sites. Such a deuteron-induced (anti)ferroelectric transition has been reported in zero-dimensional hydrogen-bonded crystals, such as BHP^{4,5} and $\text{K}_3\text{H}(\text{SO}_4)_2$.^{11,12} It should be noted that, for detecting a structural phase transition more precisely, further experiments such as heat capacitance measurements, X-ray analyses, and vibration spectra (IR and Raman) analyses in the low-temperature region are desirable. Incidentally, the magnitude of the decrease in the permittivity of the deuterated PBSQ crystal at temperatures below 28 K is less than that expected for a typical (anti)ferroelectric phase transition. This may be due to the residual quantum fluctuation of deuterons in the (anti)ferroelectric phase. A similar temperature dependence of the permittivity is found in the dielectric phase transitions of the squaric acid crystal under high pressure¹² and the partially deuterated BHP crystal.⁵

The appearance of the deuteron-induced (anti)ferroelectric phase transition suggests that the deuteron transfer takes place

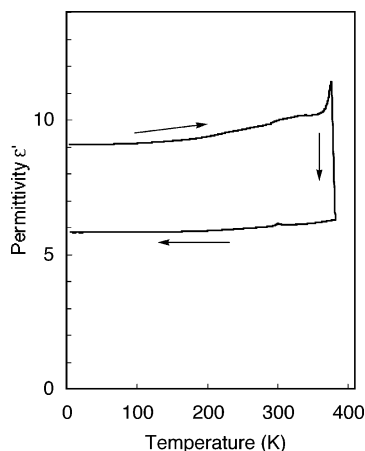


Figure 6. Temperature dependence of the ac permittivities (10 kHz) of the PBSQ crystal. The process of temperature control is shown by arrows.

along the double-well potential. On the other hand, the temperature-independent dielectric behavior of the hydrated PBSQ crystal indicates that the rate of the intermolecular proton transfer is nearly constant over the temperature range 4–300 K. The proton transfer, which is not affected by thermal energy, may be due to a tunneling effect in the double-well proton potential. Temperature-independent permittivity has been observed in inorganic dielectrics (e.g., KTiO_3 and SrTiO_3) at low temperatures^{25,26} and in the organic, zero-dimensional hydrogen-bonded crystal BHP.⁵ Such dielectric behavior may be interpreted in terms of *quantum paraelectricity*, which denotes that the (anti)-ferroelectric ordering of invertible dipole moments is suppressed by a certain quantum fluctuation,²⁵ such as proton tunneling.¹² The nearly temperature-independent dielectric behavior of the hydrated PBSQ crystal may be regarded as the first example of quantum paraelectricity originating from intermolecular proton tunneling in a one-dimensional hydrogen-bonded system.

It is possible that, in the nondeuterated crystal, the proton potential is of the single-well type, owing to the shortness of the hydrogen bond. In that case, the proton in the hydrogen bond should be broadly located in the single well, and the permittivity would be generated by a shift in the distribution of the protons in the hydrogen bonds. The permittivity of the ~50% deuterated sample increased slightly with decreasing temperature in the high-temperature region, but in the low-temperature region, the permittivity was almost constant and a phase transition did not occur (Figure 6b). These results can be rationalized as follows: in the high-temperature region, the dielectric response of the deuterons increases with decreasing thermal fluctuation of the deuterons, whereas, in the low-temperature region, the (anti)ferroelectric interaction is suppressed by the quantum fluctuations of the protons.

Estimation of the relative contribution of the dynamics of H_5O_2^+ to the permittivity is difficult, owing to the lack of anisotropic data on the permittivity. However, the proton dynamics in hydrogen-bonded squaric acid moieties and in H_5O_2^+ may be weakly correlated. It is possible that the ordering of the two kinds of protons occurs, being coupled with an (anti)-ferroelectric phase transition, because of the breakdown of the inversion symmetry.

The hydration waters (H_5O_2^+) in the crystal are stable at room temperature, but the water molecules could be removed by heating to afford neutral PBSQ solids. To examine the thermal dehydration processes, we carried out thermogravimetry and differential thermal analysis (DTA) measurements on the hydrated PBSQ crystal. We found that the mass of the hydrated

PBSQ crystal began to gradually decrease at ~320 K, followed by an abrupt decrease at 370 K, accompanied by an endothermic peak in the DTA chart. The decrease in mass corresponded to the mass of two water molecules. We measured the permittivity of $\text{PBSQ} \cdot 2\text{H}_2\text{O}$ above 300 K (Figure 6) and found that the permittivity increased abruptly at 380 K, accompanied by an increase in ϵ'' , and then dropped sharply ($\epsilon' \sim 6$). The dielectric behavior at ~390 K originated from the dehydration process. During the cooling process, the permittivity remained constant and did not recover to its original value. This result demonstrates that the dehydrated neutral PBSQ solid cannot exhibit a dielectric response, and it is further evidence that the observed response is not derived merely from an electronic polarization term but also involves an intrinsic contribution from the ionic hydrogen bonds and the protonated water dimer to the dielectric permittivity.

IV. Summary

A squaric acid derivative, PBSQ, was designed to promote proton mobility in the crystal. The $\text{PBSQ} \cdot 2\text{H}_2\text{O}$ crystal, composed of strong ionic hydrogen bonds, exhibited a nearly temperature-independent permittivity. This result contrasts with the dielectric property of the deuterated crystal, in which a deuteron-induced (anti)ferroelectric phase transition was observed. The nearly temperature-independent dielectric response of the $\text{PBSQ} \cdot 2\text{H}_2\text{O}$ crystal is the first example of quantum paraelectricity originating from the intermolecular proton transfer in a one-dimensional hydrogen-bonded system.

References and Notes

- (1) de la Vega, J. R. *Acc. Chem. Res.* **1982**, *15*, 185.
- (2) Bondybey, V. E.; Haddon, R. C.; English, J. H. *J. Chem. Phys.* **1984**, *80*, 5432.
- (3) Tanaka, K.; Honjyo, H.; Tanaka, T.; Kohguchi, H.; Ohshima, Y.; Endo, Y. *J. Chem. Phys.* **1999**, *110*, 1969.
- (4) Mochida, T.; Izuoka, A.; Sugawara, T.; Moritomo, Y.; Tokura, Y. *J. Chem. Phys.* **1994**, *101*, 7971.
- (5) Moritomo, Y.; Tokura, Y.; Mochida, T.; Izuoka, A.; Sugawara, T. *J. Phys. Soc. Jpn.* **1995**, *64*, 1892.
- (6) Matsuo, T.; Kohno, K.; Inaba, A.; Mochida, T.; Izuoka, A.; Sugawara, T. *J. Chem. Phys.* **1998**, *108*, 9809.
- (7) Matsuo, T.; Kohno, K.; Ohama, M.; Mochida, T.; Izuoka, A.; Sugawara, T. *Europhys. Lett.* **1999**, *47*, 36.
- (8) Semmingsen, D.; Hollander, F. J.; Koetzle, T. F. *J. Chem. Phys.* **1977**, *66*, 4405.
- (9) Feder, J. *Ferroelectrics* **1976**, *12*, 71.
- (10) Moritomo, Y.; Tokura, Y.; Takahashi, H.; Mōri, N. *Phys. Rev. Lett.* **1991**, *67*, 2041.
- (11) Geshi, K. *J. Phys. Soc. Jpn.* **1980**, *48*, 886.
- (12) Moritomo, Y.; Tokura, Y.; Nagaosa, N.; Suzuki, T.; Kumagai, K. *Phys. Rev. Lett.* **1993**, *25*, 2833.
- (13) Liebeskind, L. S.; Fengel, R. W. *J. Org. Chem.* **1990**, *55*, 5359.
- (14) Etter, M. C.; Urbanczyk-Lipkowska, Z.; Jahn, D. A.; Frye, J. S. *J. Am. Chem. Soc.* **1986**, *108*, 5871.
- (15) Bertolasi, V.; Gilli, P.; Ferretti, V.; Gilli, G. *Chem.—Eur. J.* **1996**, *2*, 925.
- (16) Jeffery, G. A. *An Introduction to Hydrogen Bonding*; Oxford University Press: New York, 1997.
- (17) Kuz'menko, I. V.; Zhilyaev, A. N.; Formina, T. A.; Porai Koshits, M. A.; Baranovskii, I. B. *Russ. J. Inorg. Chem. (Engl. Transl.)* **1989**, *34*, 1457 and references therein.
- (18) Patton, E.; West, R. *J. Am. Chem. Soc.* **1973**, *95*, 8703.
- (19) Gilli, G.; Bertolasi, V.; Gilli, P.; Ferretti, V. *Acta Crystallogr.* **2001**, *B57*, 859.
- (20) Mathew, S.; Paul, G.; Shivasankar, K.; Choudhury, A.; Rao, C. N. R. *J. Mol. Struct.* **2002**, *641*, 263.
- (21) Cheng, H.-P.; Barnett, R. N.; Landman, U. *Chem. Phys. Lett.* **1995**, *237*, 161.
- (22) Cheng, H.-P.; Krause, J. L. *J. Chem. Phys.* **1997**, *107*, 8461.
- (23) Yeh, L. I.; Lee, Y. T.; Hougen, J. T. *J. Mol. Spectrosc.* **1994**, *164*, 473.
- (24) Vuilleumier, R.; Borgis, D. *J. Chem. Phys.* **1999**, *111*, 4251.
- (25) Müller, K. A.; Burkard, H. *Phys. Rev.* **1979**, *B19*, 3593.
- (26) Vogt, H.; Uwe, H. *Phys. Rev.* **1984**, *B29*, 1030.
- (27) Farrugia, L. J. *J. Appl. Crystallogr.* **1997**, *30*, 565.